

On orientational relief of inter-molecular potential and the structure of domain walls in fullerite C_{60}

Julia M. Khalack,^{1,2,†} Vadim M. Loktev^{1,‡}

¹*Bogolyubov Institute for Theoretical Physics of the National Academy of Sciences of Ukraine,*

14b Metrologichna Str., Kyiv-143, 03143 Ukraine

²*Stockholm University, Arrhenius Laboratory, Division of Physical Chemistry, S-106 91 Stockholm, Sweden*

[†]E-mail: julia@phyc.su.se

[‡]E-mail: vloktev@bitp.kiev.ua

October 28, 2018

Abstract

A simple planar model for an orientational ordering of three-fold molecules on a triangular lattice modelling a close-packed (111) plane of fullerite is considered. The system has 3-sublattice ordered ground state which includes 3 different molecular orientations. There exist 6 kinds of orientational domains, which are related with a permutation or a mirror symmetry. Interdomain walls are found to be rather narrow.

The model molecules have two-well orientational potential profiles, which are slightly effected by a presence of a straight domain wall. The reason is a stronger correlation between neighbour molecules in triangular lattice versus previously considered square lattice

A considerable reduction (up to one order) of orientational interwell potential barrier is found in the core regions of essentially two-dimentional potential defects, such as a three-domain boundary or a kink in the domain wall. For ultimately uncorrelated nearest neighbours the height of the interwell barrier can be reduced even by a factor of 10^2 .

PACS: 61.48.+c, 78.30.Na

1 Introduction

An elegant hollow cage structure of the C_{60} fullerene molecule has drawn a close attention of scientists because of its unique I_h icosahedron symmetry. A nearly spherical form of the molecule leads to very unusual physical properties of solid C_{60} , fullerite.[1, 2, 3, 4] While at the room temperature the molecules can be considered to be the exact spheres, the low temperature properties of fullerite are determined by the deviation of the molecule geometry from the spherical one. At these temperatures an orientational molecule ordering takes place, which is a basic issue for understanding the results of recent He-temperature experiments on heat transport,[5, 6] linear thermal expansion,[7, 8] and the specific heat [9] of the C_{60} fullerite.

The mass centers of the C_{60} molecules in fullerite are arranged into an *fcc* structure characteristic for close packed spheres with isotropic interactions between them. At the room temperature the molecules are found to be freely rotating. The resulting crystal space group is

$Fm\bar{3}m$.

Upon the lowering of temperature, the fullerite is subjected to two transitions. At $T \approx 260$ K, it undergoes the first order phase transition, after which the *fcc* crystal lattice is divided into four simple cubic sublattices. The molecules are now allowed to rotate about one of the 10 molecular threefold axes. Other two of the three rotational degrees of freedom are frozen. Within each of the four sublattices, the allowed molecule rotation axis is fixed along one of the four ([111], $[\bar{1}\bar{1}\bar{1}]$, $[\bar{1}\bar{1}1]$, or $[\bar{1}1\bar{1}]$) threefold cubic axes, so that the crystal space group is $Pa\bar{3}$.

It is worth noting that the truncated icosahedron form of a C_{60} molecule allows for a more symmetric regular crystal structure with only one sublattice and with the four of the above mentioned molecule threefold axes oriented along the threefold crystal axes (usually regarded as a standard molecule orientation). But such a structure is energetically unfavourable for the anisotropic intermolecular interaction. Instead, the observed low-energy structure is obtained by a simultaneous counterclockwise 22° rotation of the C_{60} molecules from the initial standard orientation about their fixed $Pa\bar{3}$ threefold axes.

As a result of such a rotation, each C_{60} molecule is oriented with one of the negative charged double C=C bonds to every one of the six neighbour molecules belonging to the same close-packed (111) plane perpendicular to the molecular rotation axis. To the other six neighbours (belonging to two adjacent (111) planes) the molecule is oriented with the positive charged pentagons (P). Therefore following a commonly used notation we denote this orientation as “P orientation”. For an ideal structure with all the molecules having a P orientation, every pair of nearest neighbours is characterized with a pentagon from one molecule opposing a double bond from another molecule.

On the other hand, a potential profile of the fullerene molecule rotating about its fixed threefold axis has an additional metastable minimum¹ corresponding to 82°

¹We do not consider to be distinct the energy degenerate minima obtained by 120° rotation about the threefold molecular axis.

rotation from the standard orientation (and to 60° rotation from the P orientation). In this minimum, the molecule opposes the neighbour molecules from the same (111) plane with the double bonds, and the molecules from adjacent planes are opposed with hexagons (H orientation²). The energy difference between the P and H minima is about 11 meV (\approx 130 K) and the height of the potential barrier is 235-280 meV (\approx 2700-3200 K).[10, 11]

At the high enough temperatures, molecules are able to jump between the two energy minima due to the processes of a thermal activation. An average P/H ratio is given by the Boltzmann distribution law. Just below the high temperature phase transition ($T \approx$ 260 K) a fraction of the H oriented molecules is close to 0.5, and for $T \approx$ 90 K it tends to 0.15.[12]

For the temperatures below 90 K the situation changes drastically. A waiting time for a molecule to obtain a sufficient energy for a jump between the P and H orientations reaches the order of several days ($10^4 - 10^5$ s) or even more. Therefore at some critical temperature (its exact value near 90 K depends slightly on the cooling conditions) the molecules become frozen in their current orientational minima, and a transition to an orientational glassy phase takes place. Below this transition a fraction of H oriented molecules remains practically unchanged and equal to its equilibrium value (about 15%) characteristic for the temperature of the glass transition. In other words, in the average every 7th molecule has the H orientation, and with the very high probability every C₆₀ molecule has at least one misoriented neighbour.

While the orientational glass structure is believed to persist down to the lowest temperatures, some of the experimental data obtained at helium temperatures can not be explained with the concept of H oriented molecules alone. For example, the data on heat conductivity [5, 6] show a maximum phonon mean free path of about 50 intermolecular spacings, what implies only a 0.02 fraction of scattering ("wrong") molecules. Besides, the negative thermal expansion [7, 8] and the linear contribution to the specific heat [9, 13] of the fullerite samples at helium temperatures are explained with the help

of the tunnelling (i.e. quantum) transitions of the C₆₀ molecules between nearly degenerate orientational minima. Such a possibility was firstly assumed in Ref. [14], where all the molecules in a crystal were supposed to be in tunnelling states. However, the paper [13] accurately estimates the tunnelling frequency to be about 5.5 K, and the number of tunnelling degrees of freedom to be $\sim 4.8 \times 10^{-4}(N/60)$, where N is the number of carbon atoms in a crystal. Obviously, the number of the H oriented molecules is much bigger, and the above mentioned potential barrier between the H and P orientations is too high to provide such a low tunnelling frequency. Therefore the defect states other than the simple H oriented molecules should be considered.

One of the possibilities for a realization of the low potential barrier for C₆₀ molecule is indicated in our previous paper.[15] Relatively low barrier sites can appear within the orientational domain walls because of the superposition of the mutually compensating potential curves due to interaction with the neighbour molecules belonging to different domains. For the case of orientational ordering of hexagons on a square planar lattice considered in [15], the height of the potential barrier in the wall is found to be 5 times less than in the regularly ordered lattice. Such a lowering seems to be insufficient to provide the necessary magnitude of tunnelling frequency following from the available experimental data analysis.[13]

Meanwhile, most of the results obtained for a square lattice seem to be caused by the incompatibility of the molecule threefold C₃ symmetry axis with the lattice fourfold C₄ symmetry axis. In the case of fullerite, a fullerene molecule holds 4 threefold axes and 3 twofold axes intrinsic to the fcc lattice. Furthermore, the closest-packed (111) plane of the Pa $\bar{3}$ lattice has a hexagonal structure. Six of the 12 molecule nearest neighbours belong to a hexagonal plane, while only 4 of them belong to the same square (001) plane.

Therefore it is interesting and necessary to investigate the main features of orientational ordering for the case of the molecule symmetry identical to that of the lattice. In the present paper we are concerned with the possible orientational domain structures formed by the simple flat hexagon-shaped molecules arranged into a more relevant to a real situation hexagonal lattice, with both the molecule and the lattice symmetry axes being C₃. The main purpose of the paper is to estimate the energetic inter-molecular interaction barriers for both regular close-packed planar structure and for the vicinity of extended orientational defects.

It is a pleasure and a honour for us to devote this paper to the Ukrainian low temperature experimentalist of a world-wide reputation Prof. Vadim G. Manzhelii whose contribution to the physics of cryocrystals in general and to the physics of fullerites and fullerides in particular is well-known and can not be overestimated.

²Strictly speaking, the term 'H (or P) configuration' is more adequate for describing a mutual orientation of two neighbouring molecules. Nevertheless, for every chosen pair of neighbouring molecules (let us denote them as A and B) with the fixed directions of allowed rotation axes, the mutual orientation depends strongly only on the rotation angle of one molecule (say, A). The other molecule (B) is always (at any angle of its rotation) turned to the first one (A) with a double bond. Therefore, the interaction energy of the pair weakly depends on the rotation angle of the second molecule. As to the molecule A, it is at any rotations always turned to B with a belt of pentagons and hexagons interconnected by single bonds. Thus, namely the molecule A of the pair A,B is responsible for the mutual orientation. Aside from this, upon the rotation of the molecule A from orientation P to orientation H this molecule becomes turned with hexagons (instead of pentagons) to five more its nearest neighbours. At the same time, the energy of its interaction with the other 6 nearest neighbours remains practically unchanged, because the energy depends mainly on the orientation of that latter molecules. Basing on the reasons mentioned above, we follow the common notations and use the letters 'P' and 'H' to denote an orientation of a single molecule, while keeping in mind those 6 pair orientations for which this molecule rotation angle is crucial.

2 Model

Let us consider a system of flat hexagonal molecules³ located in the sites of a rigid hexagonal planar lattice, modelling a (111) plane of the 3D *fcc* lattice.

Following the empirical potentials used for modelling the intermolecular fullerene interaction (see, for example, Ref. [16] and references therein), we suppose two kinds of negative charges, $-(1 \pm \alpha)$, to be located at the centers of hexagon sides (see large and small filled circles in Fig. 1(a)). These negative charges recall single and double covalent bonds between carbon atoms at the hexagon edge of the truncated icosahedral fullerene molecule. Introduction of the charge parameter α reduces the C_6 hexagon symmetry down to C_3 intrinsic for real C_{60} . A requirement of electro-neutrality of the model hexagon molecule stipulates a presence of unit positive charges at its vertices (shown with the open circles in Fig. 1(a)).

For an initial orientation (an analogue of the standard orientation in fullerite) the molecules are chosen to be aligned with the positive charges along the lattice directions. The topmost (positive *Y* direction) negative charge has to be a larger one (see Fig. 1(a)). The molecule rotation angle ϕ is measured starting from the positive *X* direction.

Interaction between the two nearest molecules is given with the superposition of the Coulomb interactions between the vertices and bonds of these molecules. The exact form of the resulting interaction function can be found in Ref. [15] (Eqs.(1-4)). Interaction is multipolar, so it depends not on the difference of the molecules rotation angles only (as for the case of the spin systems with Heisenberg exchange coupling), but essentially on both the angles. So, the energy of interaction of the two neighbour molecules characterized with rotation angles ϕ_1 and ϕ_2 has to be written as $W(\phi_1; \phi_2)$. The clockwise and counterclockwise rotations have different effect on the interaction:

$$W(\phi_1; \phi_2) \neq W(-\phi_1; \phi_2) \neq W(\phi_1; -\phi_2). \quad (1)$$

On the other hand, a clockwise rotation of the first molecule is somewhat equivalent to a counterclockwise rotation of the second molecule. Hence, a combination of the lattice mirror symmetry with the molecule mirror symmetry leads to the following symmetry relation for the interaction function:

$$W(\phi_1; \phi_2) = W(-\phi_2; -\phi_1). \quad (2)$$

Rotating the molecules shown in Fig. 1(a) by an angle $2\pi/3$ (or $4\pi/3$) about a threefold axis located in the center of the triangle 123, one can find that the pair interaction of the molecules 2,3 (or 3,1) is given with the same function $W(\phi_2; \phi_3)$ (or $W(\phi_3; \phi_1)$, respectively). A

³In some sense, they can be regarded as imitating the C_{60} molecules viewed along C_3 axis. Strictly speaking, such imitation is competitive only for the fullerene molecules with the fixed C_3 axis perpendicular to the considered (111) plane. The C_{60} molecules belonging to other three $P\bar{a}3$ sublattices have their fixed threefold axes tilted to this plane.

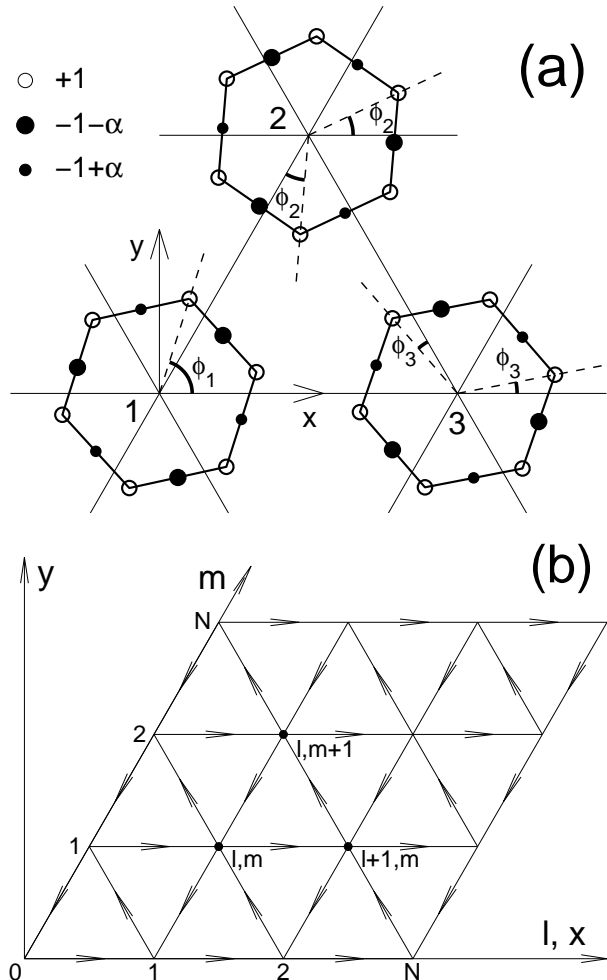


Figure 1: (a) A local geometry of the model molecules on the triangular lattice. Note that molecular rotation angles (shown with the help of dashed lines) can be measured from any of the three lattice directions. (b) A geometry of the simulation cell. Arrows give the $1 \rightarrow 2$ order of the input parameters for the pair interaction function $W(\phi_1; \phi_2)$.

relative displacement (which was vertical or horizontal in the case of the square lattice considered in Ref. [15]) of the two molecules does not have to be taken into account, but an order of the angle parameters is essential.

For a simulation of the possible domain structures, we consider a finite parallelepiped-shaped system, which geometry is shown in Fig. 1(b). It consists of 20×20 hexagon molecules labeled with the two indexes l and m . Arrows show the order of the interaction function arguments for each pair of hexagons. The system Hamiltonian then reads:

$$\begin{aligned} H = & \sum_{l,m=0}^{N-1} [W(\phi_{lm}; \phi_{l+1,m}) \\ & + W(\phi_{l+1,m}; \phi_{l,m+1}) + W(\phi_{l,m+1}; \phi_{l,m})] \\ & + \sum_{l=0}^{N-1} W(\phi_{lN}; \phi_{l+1,N}) \end{aligned}$$

$$+ \sum_{m=0}^{N-1} W(\phi_{N,m+1}; \phi_{Nm}), \quad (3)$$

where $N = 19$, and the last two terms are introduced to take into account the edge molecules. For numerical simulations, the charge parameter α is chosen to be $1/3$. A hexagon side makes 0.3 of the lattice spacing.

3 Possible ordering types

For a general case of an orientational ordering of the identical molecules on a planar hexagonal lattice, the structures with 1, 3, 4, and 7 sublattices are possible. One sublattice structure would correspond to a uniform rotation of all the molecules on a lattice. Three sublattice structure is characteristic of antiferromagnetic systems (Loktev structure [17]). A close-packed (111) plane of the $Pa\bar{3}$ structure should contain the molecules belonging to four different sublattices. The results of STM imaging of the (111) fullerite surface [18] confirm this fact.⁴ A more complicated case of seven sublattices could be expected for less symmetric molecules.

As to considered C_3 symmetric hexagons, a rather aesthetic expectation of the threefold site symmetry⁵ implies either 1 or 3 sublattice case, or a 4 sublattice structure involving three identical rotations. Numerical calculations give for a ground state a three sublattice structure shown in Fig. 2(a). It is interesting to notice that in the 3 sublattice structure the energy minimum corresponds to the molecule positions which do not provide the minimum of the pair potential. The obtained molecule rotation angles are ($\alpha = 1/3$):

$$\phi_1 = 72.37209^\circ; \phi_2 = 25.24477^\circ; \phi_3 = 10.87533^\circ. \quad (4)$$

Another possible (energy degenerate) ground state can be found with the help of the symmetry relation (2). The corresponding angles are given with

$$\phi'_1 = -\phi_1; \phi'_2 = -\phi_2; \phi'_3 = -\phi_3. \quad (5)$$

This ground state is related by the mirror symmetry to the state defined with Eq. (4).

The high symmetry of the hexagon molecules makes it difficult to perceive the ordering pattern presented in Fig. 2(a). A more complicated task of finding an orientational defect in this pattern becomes unfeasible. Therefore for the purpose of visualization, we implement a vector representation of hexagon molecules shown in Fig. 2(b). The vector rotation angle is three times a hexagon rotation angle: $\phi_{lm}^v = 3\phi_{lm}^h$. A vector can be rotated from 0° to 360° . As a result, a difference between sublattices appears to be more clear.

⁴At the beginning of the fullerene era, there were some publications [19, 20] reporting an 8-sublattice *fcc* structure for the low temperature fullerite. This structure could be obtained by division of each of the four *sc* $Pa\bar{3}$ sublattices into two *fcc* sublattices with different (P and H) molecular orientations. However, the 8-sublattice structure has not been confirmed by further investigations. Therefore, we do not consider it here.

⁵An absence of the site symmetry would induce a distortion of the lattice.

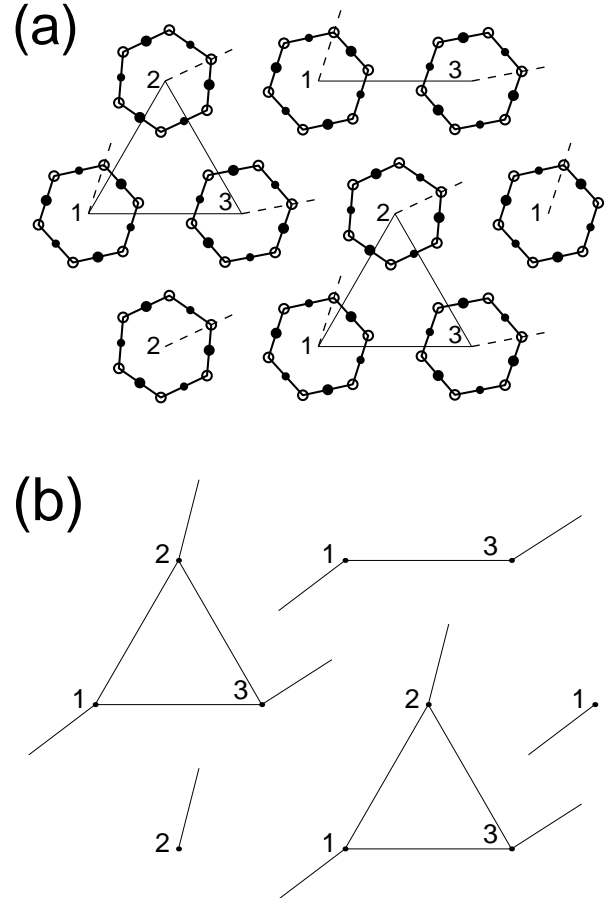


Figure 2: A ground state orientational ordering of the hexagon molecules (a), and the same ordering patterned with vectors (b).

Figure 3 shows a change of the molecule interaction energy with a change of its orientation for the three molecules belonging to three different sublattices. It is clearly seen that the molecules are not identical. All of them have double-well energy profiles, but the height of the interwell energy barrier varies by a factor of 2. The potential minima of the 2nd molecule are almost energy degenerate, the energy difference being only $1/20$ of the barrier height (situation, similar to the case of fullerite).

For a comparison, the same potential profiles are shown for the molecules from the edge of the simulated lattice (see Fig. 4). Such molecules keep only 4 of the 6 nearest neighbours (molecules from two different sublattices are missing). As a result, the overall potential profile is lowered by a factor of $6/4$. The C_{60} molecule at the fullerite (111) edge surface is missing 3 neighbours from 3 different sublattices. Therefore one could expect lowering the orientational barriers by a factor of $12/9$.⁶

⁶Nevertheless, it should be emphasized that a change (or relatively weak lowering) of inter-molecular rotational barriers appears to be too small for all the cases of the regular structure to allow for an orientational tunnelling which is necessary for a number of physical phenomena. One has to remember that the mass of the C_{60} fullerene molecule is 720 a.u. It makes very strong constraint for the height and the width of energetic barriers which are able to give an observable probability (or frequencies [13]) of orientational

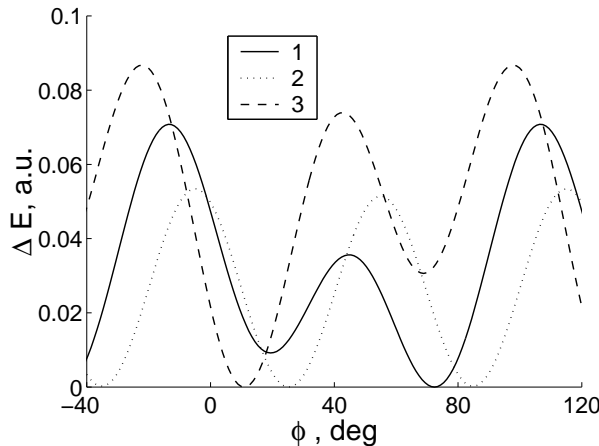


Figure 3: Orientational potential profiles for regular molecules belonging to three different sublattices.

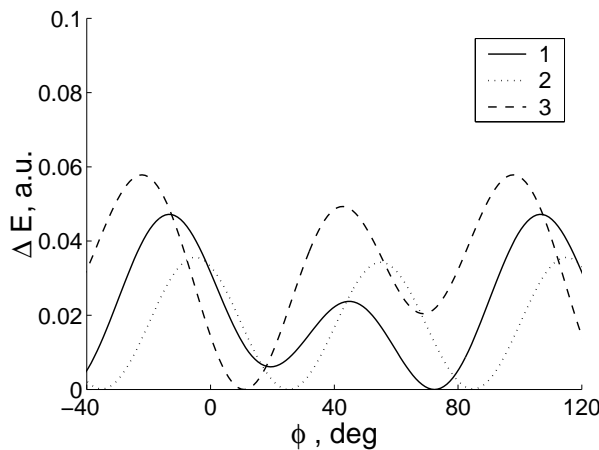


Figure 4: Orientational potential profiles for the edge molecules belonging to different sublattices.

But the real situation is even more complicated. A three-dimensional character of fullerite lattice leads to subdivision of the neighbours of an arbitrary bulk fullerene molecule into only two categories, denoted here as double-bond (to which the molecule is oriented with the double bond), and pentagon (to which the molecule is oriented with the pentagon or hexagon) neighbours. The six double-bond neighbours belong to the (111) plane normal to the molecule fixed C_3 axis. The rest six pentagon neighbours, which give a major contribution to the molecule orientational profile, are located in other (111) planes.

Therefore an edge molecule with a fixed C_3 axis normal to the edge surface misses three pentagon neighbours, while the molecules with three other directions of allowed rotation axis are missing two double-bond and one pentagon neighbour each. As a result, the potential relief of a molecule with a normal rotation axis is more shallow than the relief of other molecules. In this way, the molecules from the four different sublattices which are identical by their rotational properties in the bulk fullerite become non-identical at the edge surface crystal tunnelling transitions.

defect due to a loss of the symmetry. This non-identity evidently reveals itself in the presence of two additional lower temperature order-disorder phase transitions reported in [21].

4 Linear orientational defects

A general kind three sublattice two-dimensional triangular lattice allows for orientational ordering of three different types. Molecular orientations for these ordering types are related to each other with cyclic permutations of the rotation angles ϕ_i ($i = 1, 2, 3$, cf. Eq. (4)) for the molecules located at the vertices of a lattice triangle (eg., a triangle 123 shown with a solid line in Fig. 2). In the case of the considered hexagon molecules an existence of the mirror orientational twin defined with Eq. 5 leads to appearance of three additional ordering types, which are related to the basic permutation ones with the mirror symmetry.

As a result, the considered lattice allows for simultaneous existence of orientational domains with 6 different ordering types. A boundary between two domains contains a linear orientational defect (domain wall). Such defect can involve a permutation (clockwise or counter-clockwise) or a mirror transformation (with a center at 3 different lattice sites) of molecular orientations.⁷

A domain wall of the permutation type is presented in Fig. 5(a). The rotation angles of the molecules located at the vertices of a lattice triangle (shown with solid lines) have the values ϕ_1 , ϕ_2 , and ϕ_3 in the left domain. In the right domain they are equal to ϕ_2 , ϕ_3 , and ϕ_1 , correspondingly. The domain wall (grey) is relatively narrow. Its width (measured along the horizontal close packed l direction) is about one period of 3-sublattice structure. As seen along the close packed m direction, this defect can be regarded as obtained by removal of one element from an ideal sequence ...1231231... of molecular orientations. The resulting sequence is ...123|231....

Orientational dependence of the potential energy of the four central molecules from the domain wall is given in Fig. 5(b). The molecules are marked in Fig. 5(a) and labeled with their m index, while l is taken to be 10. Molecules 8 and 10 have the orientations of the type 2, and the rotation angles of molecules 9 and 11 are close to ϕ_3 . The potential profiles are quite close in the form to the profiles of the regular molecules (shown in Fig. 3), but one of the two potential barriers is lowered for each molecule.

Orientational domain walls of a mirror nature are wider than the permutation ones. Fig. 6(a) gives an example of the mirror domain wall. For this wall, a sequence of molecular orientations in the m direction is ...123?3'2'1'..., where a question mark stands for a molecule in the mirror plane. This molecule does not fit any regular orientation. Instead, it reflects the mirror symmetry of the wall. Figure 6(b) clearly shows the orientational potential minimum of the molecule 10 to be

⁷For the case of fullerite, there are 4+4 different ordering types and 3+4 different inter-domain boundaries (not related with the symmetry operations).

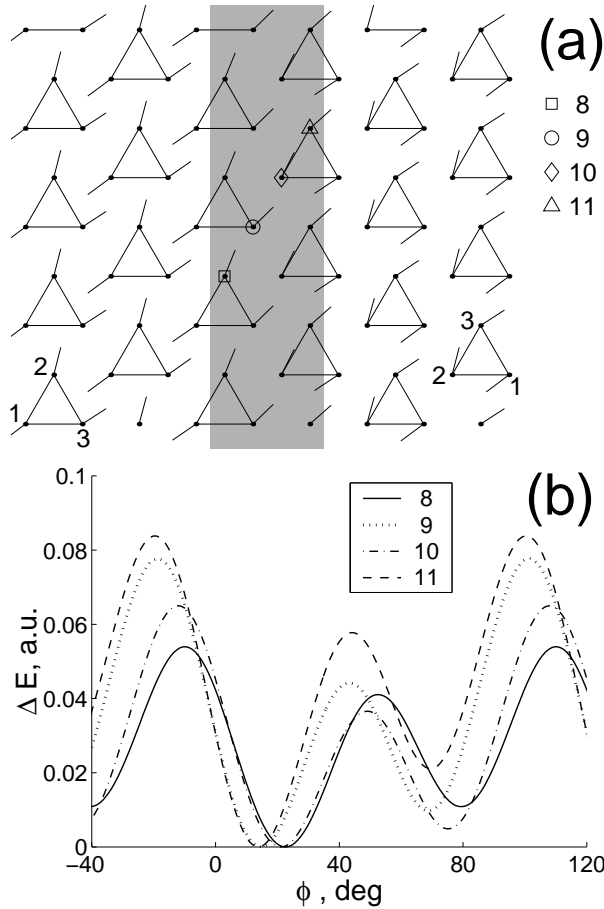


Figure 5: Permutation domain wall (a) perpendicular to close-packed row, and orientational potential profiles (b) for the four marked molecules identified with the lattice index m ($l=10$).

located at the rotation angle $\phi = 60^\circ$. Such an orientation corresponds to aligning one of the mirror planes of the hexagon molecule to the domain wall mirror plane.

The mirror symmetry of orientational defect is also manifested through the symmetry of potential curves of other molecules. The potential profiles of the molecules 9 and 11 (orientations 3 and 3'), 8 and 12 (orientations 2 and 2') are related through $\Delta E_9(\phi) = \Delta E_{11}(-\phi)$ and $\Delta E_8(\phi) = \Delta E_{12}(-\phi)$, respectively.

In the vector pattern of Fig. 6(a), this symmetry is given with the clockwise-counterclockwise vector rotations on the two different wall sides. Since the rotation angles are measured from the X direction, the vectors representing molecule 9 and 11 (8 and 12) rotations are related with the mirror plane parallel to the X direction.

The effect of the domain wall on the potential relief of the molecules 8 and 12 (orientations 2 and 2') is found to consist in a slight lowering of one of the two barriers. For the molecules 9 and 11 (orientations 3 and 3') close to the center of the domain wall, both the potential barriers are lowered considerably. But the position and the relative height of the secondary minimum are unchanged, resulting in a shallow character of this minimum seen in Fig. 6(b).

The domain walls given in Figs. 5, 6 have their di-

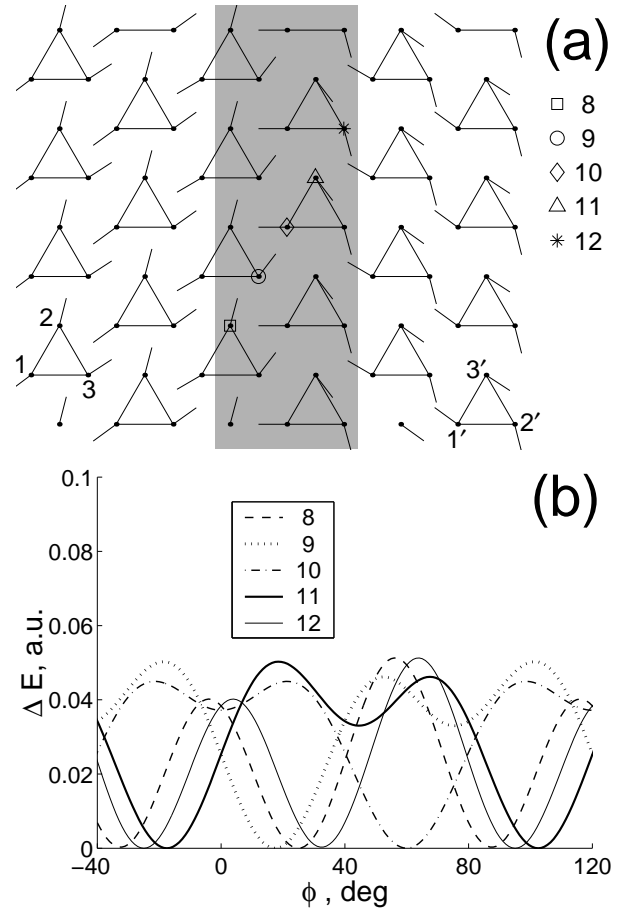


Figure 6: Mirror domain wall (a) perpendicular to close-packed row, and the potential profiles (b) for the five marked molecules with $l=10$ and with the indicated m value.

rections parallel to one of the sublattice period vectors, and perpendicular to one of the close-packed molecular row directions. At the same time, there is a possibility for a domain wall to lie along the close-packed molecular rows. An example of a permutation domain wall of this kind is presented in Fig. 7(a). The relationship between the left and right domains here is the same as in Fig. 5, but the location of the domain wall line is different. As a result, the molecular orientation sequence along the m molecular row can now read $\dots 231|312 \dots$ ($l=8$), $\dots 312|123 \dots$ ($l=9$), or $\dots 123|231 \dots$ ($l=10$). Therefore, the central part of the domain wall contains molecules with 6 different potential profiles (orientations 1, 2, and 3 from the left domain, and orientations 3, 1, 2 from the right domain). The three potential profiles with the lowest energy barriers are shown in Fig. 7(b). Noteworthy that here we gain a low barrier profile with almost energy degenerate minima (see dotted curve).

A mirror nature domain wall parallel to close-packed molecular row has a more complicated structure shown in Fig. 8(a). It is again wider than the permutation wall, so that the molecules from *three* close-packed rows have substantially corrupted orientational potential relief. As a result, the number of intra-wall molecules with different orientational profiles increases up to 9, opposed to

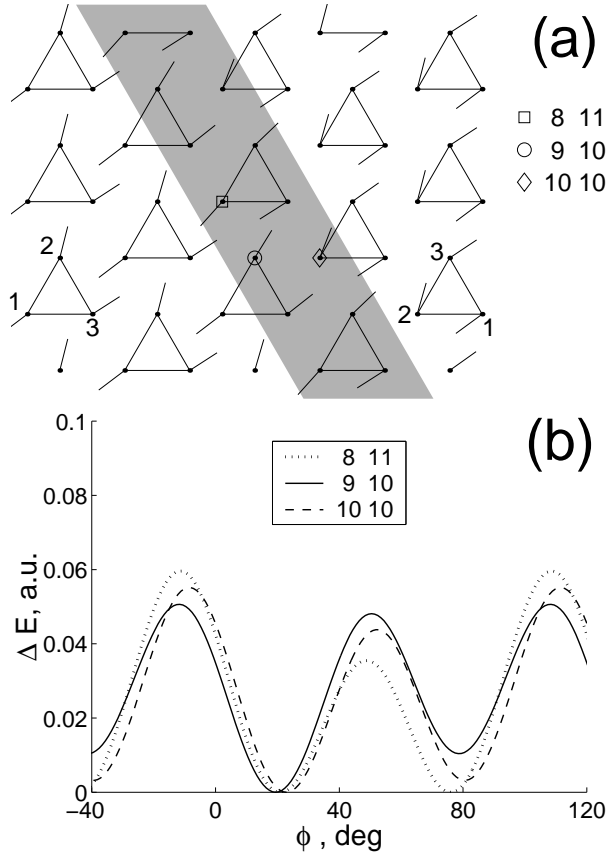


Figure 7: Permutation domain wall parallel to close-packed row (a), and orientational potential profiles (b) for the marked molecules with the given lattice indexes l and m .

6 different profiles for a permutation wall. Furthermore, the direction of the domain wall does not coincide with the lattice mirror plane, so there are no mirror symmetry in the pattern of Fig. 8(a), and, respectively, no symmetry relations for the potential curves (conf. the mirror symmetry of the potential profiles shown in Fig. 6(b) for the domain wall perpendicular to close-packed molecular row). In Fig. 8(b) we give the orientational potential profiles for the three molecules with the lowest interwell energy barriers. It is seen that there exists a molecule (o) which interwell barrier is about 1.4 times lower than the lowest of the regular molecules interwell barriers. The molecule is situated in the center of the domain wall and marked with a circle. The corresponding potential profile is plotted with a solid line in Fig. 8(b). The obtained reduction of the orientational interwell barrier is caused by a less correlation between the nearest neighbour molecules (every molecule within the considered wall has neighbours of six different orientations).

5 Two-dimensional defects

The results on the modelling of the straight domain walls in the considered system show that the molecules with the most shallow potential profile tend to appear at sites with the reduced correlation between the orientations of

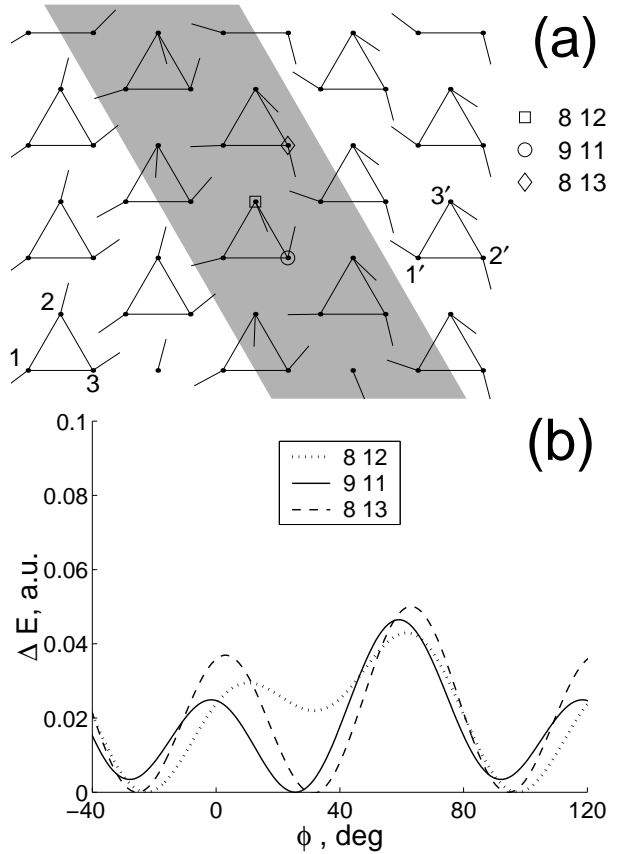


Figure 8: Mirror domain wall parallel to close-packed row (a), and the potential profiles (b) for the marked molecules (lattice indexes l and m are indicated).

the neighbour molecules. For the straight walls such condition is met at the boundary of two domains with different sets of equilibrium molecule orientations (mirror domain walls).

Then it is straightforward to continue the search for the shallow potential molecules in the core regions of essentially two-dimensional orientational defects. One of such promising two-dimensional defects is a meeting point of three different domains. Molecules at the center of this defect should have three pairs of neighbours belonging to three different domains, so one could expect for an additional decrease of interwell barriers with respect to the two-domain boundary case.

The results of numerical calculations indeed show the further reduction of interwell potential barriers at the boundary of three orientational domains. The most effective reduction is found to take place in the presence of mirror boundaries.

Figure 9(a) shows an example of orientational defect formed at the intersection of three domain walls perpendicular to molecular rows. The left (narrow) domain wall is of a permutation type, the other two (the bottom one and the right one) have a mirror nature and are much wider. The right domain wall incorporates a kink in order to minimize a surface spanned by the defect. Molecules with the lowest interwell barriers are marked.

As it is mentioned above, no significant potential

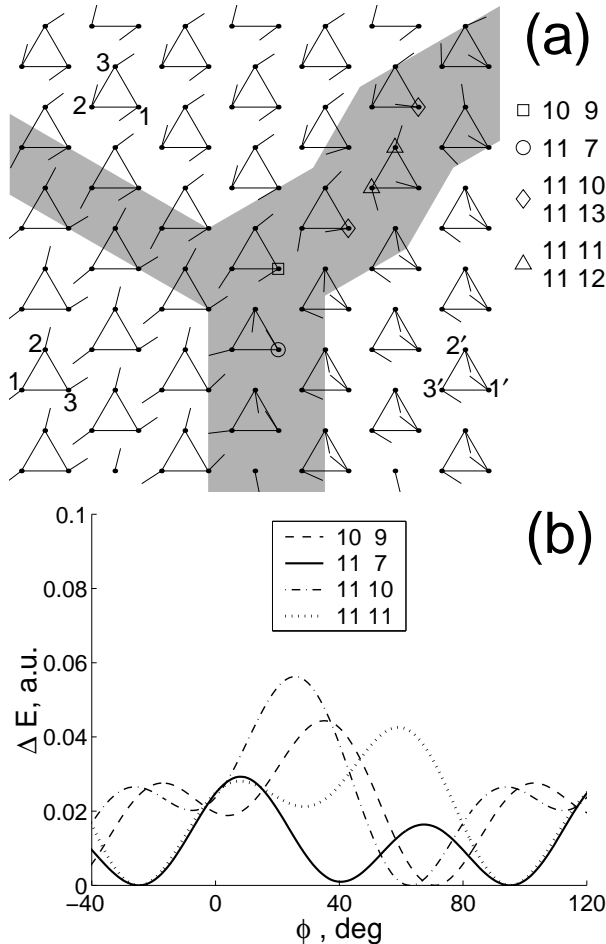


Figure 9: Structure of orientational defect (a) formed at the boundary of three orientational domains, and the potential profiles (b) for some chosen molecules in the defect core region. Pairs of molecules marked with the same sign (\triangle or \diamond) have the symmetry related potential profiles, so only one of the profiles is given for each pair. Molecules are labeled with l and m indexes.

barrier reduction has been observed for straight domain walls perpendicular to close-packed molecular rows. Therefore the marked molecules can be seen only at the crossing of the three walls. The corresponding orientational potential profiles are plotted in Fig. 9(b).

It is surprising that the potential profile with the least energy barrier belongs not to the molecule \square situated in the very center of the defect (potential curve plotted with a dashed line) with totally different orientations of all the 6 nearest neighbours, but to the molecule located at the beginning of the bottom domain wall (o , solid line). For the last molecule the orientations of the nearest neighbours differ only slightly from that in the straight wall, but the interwell potential barrier is 2.3 times lower than the lowest regular molecule barrier.

The other four molecules which are marked in Fig. 9(a) are located within the center of the kink in the right domain wall. At a closer look, one can find a kind of a symmetry center at the middle of the line between the molecules marked with \triangle . An exact symmetry is following: if the centers of two molecules are related

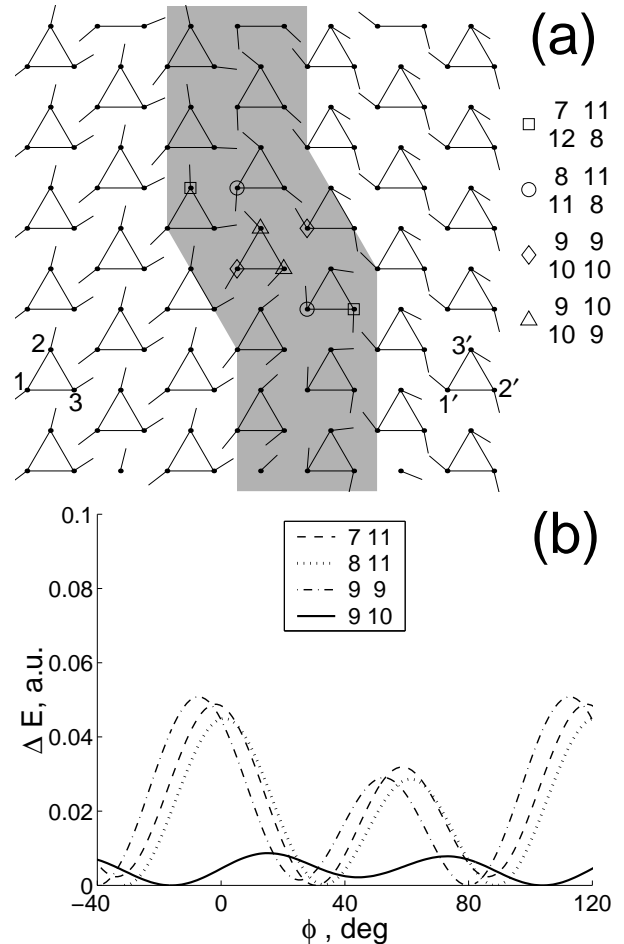


Figure 10: The structure of the kink in the mirror domain wall (a), and orientational potential profiles (b) for marked molecules. Only one potential curve is given for every pair of symmetry related molecules which are marked with identical signs. Indexes 1 and m are indicated.

with inversion symmetry, these molecules have the rotation angles which have equal absolute values, but different signs. Therefore the two molecules marked with \triangle (as well as the two molecules marked with \diamond) have the same orientational dependence of intermolecular interaction potential, the only difference being in the clockwise or counterclockwise direction of molecule rotation. This can be compared to the symmetry of potential curves in Fig. 6(b), but there is no mirror plane in the present case. To avoid having a very complicated picture, only one of the two symmetry related curves is shown in Fig. 9(b) for each pair of molecules. Both the dotted and the dash-dotted curves have an interwell energy barrier which is less than the lowest energy barrier characteristic for regular molecules. This means that at the center of the kink in a domain wall (also a two-dimensional defect) molecules have ill-correlated nearest neighbours. Therefore the case of a kinked domain wall has to be investigated more thoroughly.

Figure 10(a) shows a structure of the kink which contains the molecule with the lowest height of the orientational interwell barrier obtained in our simulations. This

molecule (in fact, two molecules, since the kink has a center of symmetry of the described above kind) is located at the very center of the kink, and the corresponding potential curve is shown in Fig. 10(b) with a solid line. The height of the interwell potential barrier is already 5 times less than for the case of regular molecules.

6 Totally uncorrelated neighbourhood configuration

The three-dimensional defect structure of the real fullerite can be even more complicated. As a result, some molecule can have the neighbours which orientations are fixed by different elements of the defect network. In the frame of our simple two-dimensional model such neighbourhood would be totally uncorrelated, and the height of the interwell barriers could be further lowered. Therefore it is interesting to know a minimum possible height of the molecule interwell potential barrier for an arbitrary orientational configuration of its neighbour molecules.

For this purpose, let us consider a system of 7 hexagon molecules located at the sites of hexagonal lattice, so that one central molecule has 6 nearest neighbours. Rotation angles of the outer molecules are fixed to be equal to 6 random numbers between 0° and 120° , and then the orientational potential profile of the central molecule is calculated. Configurations with the most shallow potential profiles obtained in the course of about 10^6 different realizations of random neighbourhood configuration are shown in Figs. 11, 12, and 13.

Figure 11 gives an example of a molecular configuration with interwell potential barriers of a central molecule reduced by two orders of magnitude with respect to the case of totally orientationally ordered lattice. This configuration is nearly symmetric (the outer molecules have rotation angles about $\pm 30^\circ$). The central molecule has a four-well orientational potential profile with the main minimum located close to 30° . One could expect that a completely symmetric configuration might have even more shallow potential profile of the central molecule, because of the increase of the interaction energy at the minima of the potential. Contrary to the expectations, the exactly symmetric configuration (not shown) has an order of magnitude higher interwell barriers than the one shown in Fig. 11. Thus, interwell barriers prove to be extremely sensitive to even very small rotations of the molecules.

The case of the molecular configuration with a two-well orientational profile of the central molecule is presented in Fig. 12. If one does not take into account the difference between the values of negative charges, this configuration seems to be close to having a mirror symmetry. Probably, namely this difference leads to an increase of the interaction energy at the potential minima.

The molecular configuration with the lowest obtained interwell potential barrier of the central molecule (shown in Fig. 13) has no symmetry at all. The orientational profile has three minima of different depth, while the

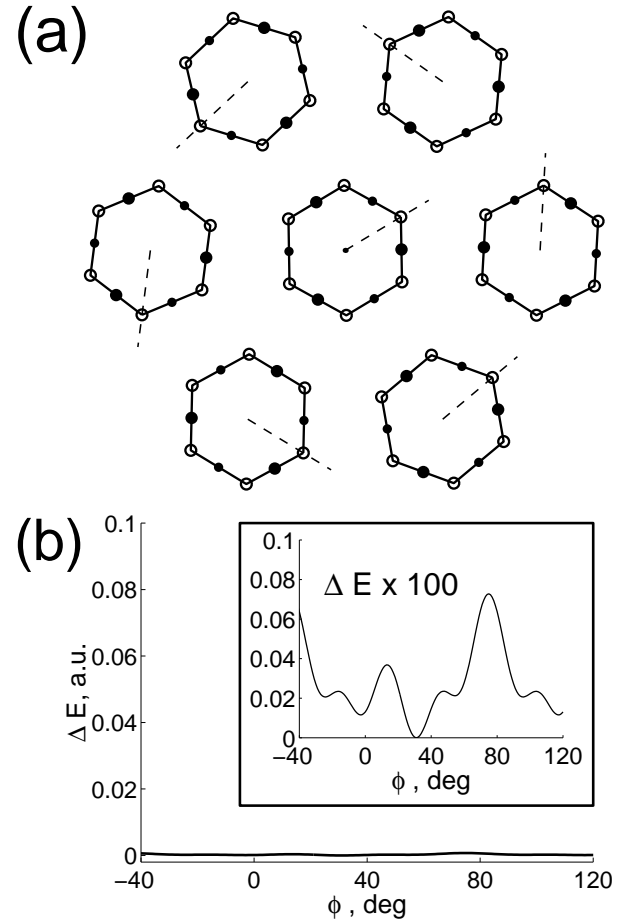


Figure 11: A molecular configuration with nearly symmetric orientations of the outer molecules (a) and the corresponding shallow potential profile of the central molecule (b). An inset in the bottom panel shows a magnified potential curve.

lowest interwell barrier is about 200 times lower than the corresponding lowest barrier in the regularly ordered lattice.

Also it should be noted that the molecules of the regularly ordered lattice (namely, the molecules with the ϕ_1 orientation, see Fig. 3) have the neighbourhood configuration with the highest possible interwell potential barrier. While minimizing the overall interaction energy, this configuration minimizes also an interaction energy at the minimum of the one molecule potential, and deepens this minimum.

7 Discussion

The considered simple planar model recovers some of the features of the fullerite lattice. First of all, it predicts a multi-sublattice structure for a system which would be arranged into a more symmetric 1-sublattice manner in the absence of anisotropic intermolecular interactions.

Then, the model involves lowering of orientation potential relief of the molecule at the crystal surface. This can be compared favourably to the absence of H oriented

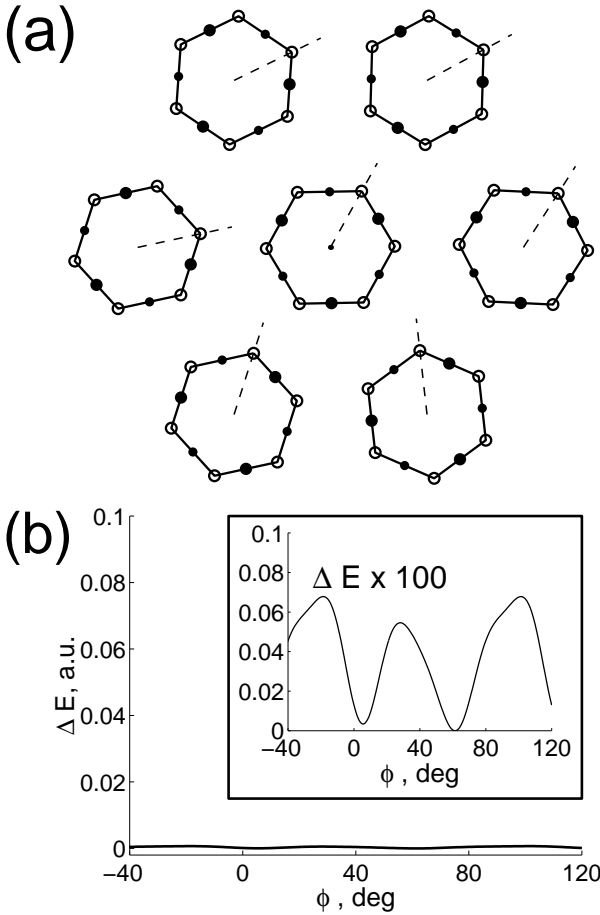


Figure 12: The same as in Fig. 11: Another nearly symmetric configuration with a two-well potential profile.

molecules at the STM image of the fullerite surface.[18] Furthermore, at a closer look this image shows a slight difference in orientations of the fullerite molecules belonging to the three sublattices which have the molecular C_3 rotation axes not perpendicular to the surface. This difference is due to a competition of the two-dimensional character of a surface (with probably another subdivision into sublattices) with the bulk equilibrium orientations of the molecules below the surface molecular layer.

Rather narrow character of the domain walls in the considered high-symmetry system is rather natural for a system with only one kind of interaction involved.⁸ It agrees well with a very sharp character of a domain wall observed in a two-dimensional monolayer of C_{60} fullerene molecules.[22] This wall contains also a very sharp kink, which is a kind of essentially two-dimensional defect that can incorporate molecules with low orientational interwell barriers.

The sharp character of the observed kink implies a possibility of existence of strongly localised orientational defects also in the bulk of the three-dimensional fullerite.

⁸For the case of ferromagnets the domain wall width is of the order of $a\sqrt{J/A}$, where a is a lattice spacing, J is an exchange, and A is an anisotropy. Since A is a relativistic correction, the ratio J/A can be increased up to 10^6 . But for the present case of one interaction this ratio is about 1.

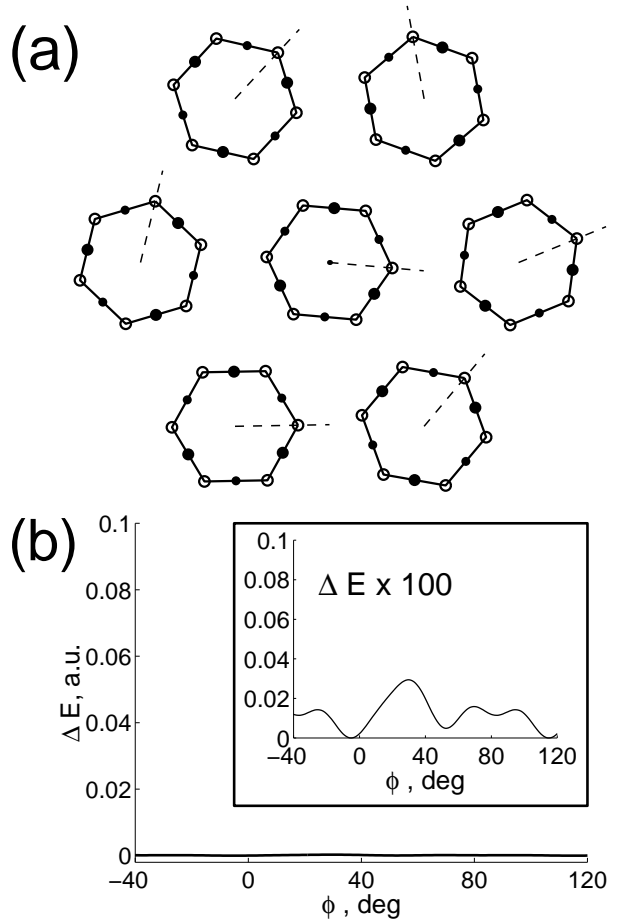


Figure 13: The same as in Fig. 11: Nonsymmetry configuration with the lowest found interwell barriers.

Some of this strongly localised defects with necessarily uncorrelated orientations of the neighbour molecules orientations should involve molecules with an orientational potential which is sufficiently shallow to give a reasonable frequency of tunnelling transitions. As to the rather high C_{60} molecule mass, the recent molecular dynamics simulations on the dislocation kink tunnelling[23] in Ag show an efficiency of tunnelling of complex heavy object under certain conditions.

The idea to explain negative thermal expansion of solids with the double-well tunnelling statistics was suggested by Freiman in 1983 for the case of solid methane.[24] In the range of temperatures where the conventional phonon mechanism does not work the thermal expansion is established as a result of competition of two factors. The first factor is a lattice contraction due to the process of populating the tunnel states with an increase of temperature. Shrinking the distances between molecules increases the height of the orientational interwell barriers, what leads to a decrease of the tunnelling energy splitting, and as a result to a decrease of the system free energy. The contraction of the lattice is stabilised by an increase of an elastic part of the free energy for every fixed value of crystal temperature.

Since the population of tunnel states has very strong exponential temperature dependence, the thermal ex-

pansion resulting from the competition of the two factors is always negative. At $T \approx 0$ K it is practically absent (no molecules on excited tunnel levels). With an increase of temperature the population of the excited state grows, therefore the lattice is contracted. But at $T > \Delta$, where Δ is the tunnel state energy splitting, both the ground and the excited states become almost equally populated, so that the effect becomes much less pronounced. This means that there should exist a maximum in the magnitude of the negative thermal expansion coefficient.

With a simple differentiation of expression (6) of Ref. [24] one can obtain that this maximum takes place at the temperature T_{\max} satisfying the equation

$$2T_{\max}/\Delta = \tanh(\Delta/2T_{\max} + 1/2 \ln(f_1/f_2)),$$

where f_1 and f_2 are the degeneracies of the ground and the excited states, respectively. It is easy to see that $T_{\max} < \Delta/2$ holds for any ratio f_1/f_2 .

Therefore the tunnelling energy splitting in fullerite can be estimated from the T_{\max} position in Refs. [7, 8] to be more than 8 K. On the other hand, the positive thermal expansion of pure fullerite at $T < 2$ K implies a presence of processes other than two-well tunnelling (probably, the conventional phonon mechanism is still valid) at this low temperature.

The possibility to detect experimentally the negative contribution to thermal expansion due to the tunnelling objects depends strongly on the relative magnitude of the positive (conventional) and negative (tunnelling in this case) contributions. In the case of fullerite, the negative contribution is more pronounced, but one still encounters a difficulty in determining the tunnelling object. The first hypothesis about a tunnelling of regular C_{60} molecules between P and H orientations [14] had a drawback of high interwell potential barrier. Further introduction of the idea of competition of isotropic and anisotropic parts of intermolecular interaction potential (though in orientational glass) [25] has lead to a current understanding (given in our previous paper [15] and the present one) that the tunnelling objects are to be found at the strongly localised orientational defects of the fullerite structure. The more detailed description of such defects could be obtained with the help of more realistic three-dimensional modelling of the C_{60} crystal structure, what should be a subject for future studies.

Acknowledgments

We would like to thank Profs. A.S.Bakai, Yu.B.Gaididei, M.A.Ivanov and V.G.Manzhelii, as well as Dr.A.N.Alexandrovskii for valuable and critical discussions. The paper is partly supported by the Program "Investigation of Fundamental Problems and Properties of the Matter on Micro- and Macrolevels" of the National Academy of Sciences of Ukraine, by the INTAS Foundation under Grant INTAS 97-0368, and also by the project N 2669 "Structure and plasticity of fullerite" of Science and Technology Center of Ukraine.

References

- [1] V.M. Loktev, *Fiz. Nizkikh Temp.* **18**, 217 (1992) [*Low Temp. Phys.* **18**, 149 (1992)].
- [2] A.P. Ramirez, *Condens. Matter News* **3**, 6 (1994).
- [3] O. Gunnarsson, *Rev. Mod. Phys.* **69**, 575 (1997).
- [4] H. Kuzmany, B. Burger, and J. Kürty, in *Optical and Electronic Properties of Fullerenes and Fullerene-based Materials* / Ed. by J. Shinar, Z.V. Vardeny, and Z.H. Kaffafi (Marsel Dekker, New York, 2000).
- [5] V.B. Efimov, L.P. Mezhov-Deglin, and R.K. Nikolaev, *JETP Lett.* **65**, 687 (1997).
- [6] V.B. Efimov, L.P. Mezhov-Deglin, *Physica B* **263-264**, 705 (1999).
- [7] A.N. Aleksandrovskii, V.B. Esel'son, V.G. Manzhelii, A.V. Soldatov, B. Sundquist, and B.G. Udovaldchenko, *Fiz. Nizkikh Temp.* **23**, 1256 (1997) [*Low Temp. Phys.* **23**, 943 (1997)]; *ibid.* **26**, 100 (2000) [**26**, 75 (2000)].
- [8] A.N. Aleksandrovskii, V.G. Gavrilko, V.B. Esel'son, V.G. Manzhelii, B. Sundqvist, B.G. Udovaldchenko, and V.P. Maletskiy, *Fiz. Nizkikh Temp.* **27**, 333 (2001) [*Low Temp. Phys.* **27**, 245 (2001)]; *ibid.* **27**, 1401 (2001) [**27**, 1033 (2001)].
- [9] J.P. Olson, K.A. Topp, and R.O. Pohl, *Science* **259**, 1145 (1993).
- [10] R.C. Yu, N. Tea, M.B. Salamon, D. Lorents and R. Malhotra, *Phys. Rev. Lett.* **23**, 2050 (1992).
- [11] S. Savin, A.B. Harris and T. Yildirim, *Phys. Rev. B* **55**, 14 182 (1997).
- [12] M. David, R. Ibberson, T. Dennis, and K. Prassides, *Europhys. Lett.* **18**, 219 (1992).
- [13] S.P. Tewari, P. Silotia, and K.Bera, *Solid State Comm.* **107**, 129 (1998).
- [14] M.A. Ivanov, V.M. Loktev, *Fiz. Nizk. Temp.* **19**, 618 (1993) [*Low Temp. Phys.* **19**, 442 (1993)].
- [15] V.M. Loktev, Yu.G. Pogorelov, Ju.N. Khalack, *Fiz. Nizk. Temp.* **27**, 539 (2001) [*Low Temp. Phys.* **27**, 397 (2001)].
- [16] P. Launois, S. Ravy, and R. Moret, *Phys. Rev. B* **55**, 2651 (1997).
- [17] V.M. Loktev, *Fiz. Nizk. Temp.* **5**, 295 (1979) [*Sov. J. Low Temp. Phys.* **5**, 142 (1979)].
- [18] H. Wang, C. Zeng, B. Wang, J.G. Hou, Q. Li, J. Yang, *Phys. Rev. B* **63**, 085417 (2001).
- [19] G. Van Tendeloo, S. Amelinckx, M.A. Verheijen, P.H.M. van Loosdrecht, G. Meijer, *Phys. Rev. Lett.* **69**, 1065 (1992).
- [20] E.J.J. Groenen, O.G. Poluektov, M. Matsushita, J. Schmidt, J.H. van der Waals, G. Meijer, *Chem. Phys. Lett.* **197**, 314 (1992).
- [21] C. Laforge, D. Passerone, A.B. Harris, P. Lambin, E. Tosatti, *Phys. Rev. Lett.* **87**, 085503 (2001).
- [22] J.G. Hou, J. Yang, H. Wang, Q. Li, C. Zeng, l. Yuan, B. Wang, D.M. Chen, Q. Zhu, *Nature* **409**, 304 (2001).
- [23] T. Vegge, J.P. Sethna, S.A. Cheong, K.W. Jacobsen, C.R. Myers, D.C. Ralph, *Phys. Rev. Lett.* **86**, 1546 (2001).
- [24] Yu.A. Freiman, *Fiz. Nizk. Temp.* **9**, 657 (1983).
- [25] V.M. Loktev, *Fiz. Nizkikh Temp.* **25**, 1099 (1999) [*Low Temp. Phys.* **25**, 823 (1999)].